.

.

Thesis To Applied for the Grade of Master of Science in Applied Physics

Albert-Ludwigs-Universität Freiburg
Faculty of Physics

Single Shot correlation in VMI- TOF measurements on He nanodroplets at MIR femtosecond laser pulses

Presented by Cristian Enrique Medina Hernandez
Date 15. febrary 2019
Referent Prof. Dr. Marcel Mudrich and Prof. Dr. Frank Stinkermeier

Abstract

In this thesis a new data acquisition method is explained for correlate single shot VMI-TOF measurements on He droplets ionized by a MIR femtosecond laser. Until now VMI images and TOF data are always treated in a statistical way. Whit these new method we expect to have some better correlation for single explosion and relate each of the event from a individual way, having specific information that could be lost in the statistical method. The correlated data is acquired by triggering the VMI camera and the TOF oscilloscope with the laser trigger, so both acquisitions begging and end after the same laser pulse. Results for the energies.....here a resumy of the results.....

Contents

0.1 Introduction 5

1 Theoretical Background **7**

1.1 Helium Nanodroplets 7

1.1.1 He Nano droplets production 8

1.1.1.1 Helium Droplets 8

1.1.1.2 Composite Clusters 12

1.2 Cluster-Intense Fields Interaction 14

1.2.1 PhotoIonization for single atoms 14

1.2.2 Multhiphoton and tunelling Ionization 16

1.2.3 kelysh Theory 18

1.2.4 Ponderomative enery 19

2 Bibliography **24**

List of abbreviations

ATI	above threshold ionization
BSI	barrier suppression ionization
CCD	Charge-coupled Device
CPA	Chirp Pulse Amplification
CWL	Central wavelength
EM	Electro Mechanics
LASER	Light Amplification by Stimulated Emission of Radiation
LT	Langmuir-Taylor
MCP	Micro Channel Plate
NIR	Near Infrared
pBASEX	polar Basis Set Expansion
PID	Proportional – Integral – Derivative
TBR	Three Body Recombination
TOF	Time of flight
VMI	Velocity Map Imaging
VUV	vacuum ultra violet
XUV	Extreme ultraviolet

0.1 Introduction

Physicists have always wonder to explain and resolve dynamic processes in short scale times, so initial conditions of processes can be describe in a time evolution scale. Describe any system like this requires to acquire data in shorter windows of time, for example a film is only a consecutive sequence of photographs that recreate a large time laps in a smaller time scale pics. For atomic physics, we are talking about a micro-cosmos that varies from microseconds, i.e several bodies dynamics, to attoseconds for atoms,where time scales can go down to 10^{-9} s, requiring to create measurement methods capable to record in shorter time, while the experiment have to be done in a controllable way to ensures its reproductivility, as any scientific method.

The time window of dynamics of a sytem is related to quantum dynamics, in a simple view also to its size. For dynamics happening in a molecule or a many body system interaction, the time window can oscillate between microseconds to fentoseconds, although for millielectronvolt-scale (meV) energy spacing of vibrational energy levels implies that molecular vibrations occur on a time scale of tens to hundreds of femtoseconds. The motion of individual electrons in semiconductor nanostructures, molecular orbitals, and the inner shells of atoms occurs on progressively shorter intervals of time ranging from tens of femtoseconds to less than an attosecond. Motion within nuclei is predicted to unfold even faster, typically on a zeptosecond time scale.

To achive this higth resolution in space and time physicist have challenged to create systems with a well controlled spatial and temporal gradient. Fortunately nowadays, laser pulses can research up to extreme non-linear optical processes, producing single aisolated pulses of ultra violet(UV) waves as short as 67 as [44]. Such fast pulses open up the possibility of time resolved measurements fort short processes like electron dynamics. However, to do this, experimental schemes must be devised that allow these new light sources to be used to perform measurements on the microcosmos. In particular, in the last few years, many studies at atom- and molecule-clusters had been published, From mid-infre red (NIR) interaction to UV or XUV pulses, that not just lead to a broad spectra to study but also to a large range of possible applications such as the generation of energetic electrons and ions in the keV-regime [11], as well as intensive XUV and attosecond pulses [35]. Laser pulses with peak intensitiesof up to 10^{21} W/cm^2 are available nowadays [28] commercially so the difficulty and expensive of the experiments source also are easy.

But this is never enough, Lasers is just one huge step in order to control and ignite atomic processes in controlled standard. Other step needed is how to acquire the

information we want. For this purpose several techniques are available depending the nature of the process. For this particular work we are interested in two techniques, Velocity map image (VMI) and Time of flight (TOF). Since its invention, this techniques has become two of the most commune and important measurement techniques in high energies physics. But detecting a signal is just one part of the job, the new laser advances like the generation of coherent high-intensity laser pulses with intensities up to $10^{22} W/cm^2$ allow multiphoton ionization that allows to get time resolved measurements. These advances have enabled the development of new research areas, as well as the investigation of ultrafast dynamics in highly excited matter to nanometer size.

In this thesis we focus our efforts on the ionization process by Mid Infrared (MIR) femtosecond pulses in doped He clusters. The interaction of the dopant with the Laser field result in a energy transfer to the droplet that ignite a ionization process, known as a nanoplasma. This resonant interaction of the laser field with a collective oscillation of the electrons in the plasma is driven by the laser field [11]. This process, caused predominantly by electron impact ionization, makes an avalanche-like ionization of the atoms in the cluster, leading to a heating of the plasma and, as a result, to hydrodynamic expansion and Coulomb explosion. To the analysis of this process we studied the electrons as well as the ion's resulting in the coulomb explosion. A velocity map imaging and a Time of flight technique are set up in parallel to acquire the data and reconstruct the initial energies and configuration of the plasma in study. In the First chapter we will present a brief introduction to the Droplet He generation, a short plasma interactions as a basic background of coulomb ionization in order to understand the physical meaning. In the second chapter a more detailed explanation of the set-up used is done. Showing from the creation of the He droplets process to its detection , going thorough the doping, and ignition process. For the third chapter a detailed explanation on the correlation method for the VMI-TOF measurements is done, and showing the set-up of the data acquisition and its advantages. In the fourth chapter we present the correlated data and its analysis. Finally the last chapter we present the conclusion of the experiment itself also as the data analysis and future works will needed to improve this process as well.

1 Theoretical Background

In this chapter we will present all the theoretical background necessary for the development of this project, from the theory and creation of the He droplets to the physics behind the plasma and coulomb explosion process to the detection techniques. In order to guide the reader in an organised way, the chapters are organized in a way that follow the processes necessaries to the performance of the experiment. this means that all the chapters explained in here occurrence in the same order during the experiment.

1.1 Helium Nanodroplets

The combination of cryogenic matrix isolation, discovered in 1954 [43], and the now well defined properties of Helium (He), specially its superfluidity face discovered in 1937 by *Kapitza et. all* [20], have as consequence one of the most powerful and flexible tool in physics, the helium nanodroplets. Helium nanodrops have unique properties that makes it very suitable for the cluster and nanophysics experiments in the last decades. For example, they do not exhibit any optical transitions in the entire infrared, visible and ultraviolet range. They can readily pick up atoms and molecules and form complexes from the species embedded in their interiors, or on their surfaces and act as a ideal matrix for atom, molecules and clusters isolation. [36] [41]. The size of a He cluster can go from of a few thousands up to 10^8 of atoms, and reach temperatures at ultra cold temperature regime (close to $0.37K$ [40]) [10]. Two main advantages of this cooling properties arise. First, dopants in the He nanodroplet are set to their absolute vibronic ground states, avoiding all other possible espectra and stablishing the cluster in a specific state, more important, the fast cooling helps to the formation of isomers that are difficult or impossible to generate with other methods [29]. Second, because the superfluid fase of the He nanodroplets [14], the bond between dopants and He is weak. Therefore, in contrast to spectroscopy in other matrices with higher temperatures, the optical transitions of many dopants are barely influenced by the He matrix [41]. The theory of He superfluidity will not be part of this section, this imformation is well documented in

other sources, and here we are based on ref. [10] where all theory is well presented to the reader. In the next section we will dedicate a bigger effort on explain the theoretical and technical background of the He nanodroplets creation as well as the physical and technical process to doped it.

1.1.1 He Nano droplets production

At room temperature, helium is a light inert gas. It is odorless, colorless, tasteless, and after hydrogen, the second most abundant element in the universe. [10]. It have a simple 2 atoms structure, exhibing numerous exotic phenomena whose theoretical descriptions are rather complex in many cases, i.e it characteristics of a quantum fluid. From helium exist two stable isotopes ^3He and ^4He. ^4He has two electrons, two protons and two neutrons, no nuclear spin and no total spin, pertaining to the bosonic family, while ^3He with only one neutron has a spin of $I = 1/2$ and belongs to the fermions [3].

The bosonic state $_4He$ is specially of interest, at temperature T$\leqslant$2.8K and under normal pressure has a phase transition from "normal liquid" He-I to super liquid He-II [38], in which the helium can be described by a Bose-Einstein condensation. Even the fermionic ^3He exhibits this phase transition at T$\leqslant 0.03K$ [17].

The superfluidity of $He - II$, at temperatures close to absolute zero, brings with it some unique features. The essential Properties for this include an almost disappearing viscosity in the superfluid phase, weak interaction, very efficient cooling, and the Transparency for electromagnetic radiation up to wavelengths in vacuum ultraviolets (VUV) Spectral range [10]. Helium has therefore in the complete visible spectrum no transitions from the ground state. Through the noble gas configuration, helium has a spherically symmetrical electron distribution [26], it can hardly be polarized and is the least reactive of all the elements.

1.1.1.1 Helium Droplets

The production He droplets had to overcome first one principal problem, its liquefaction. At the end of 19th century many gases were liquefied for the first time by applying pressure at room temperature. However, for He and hydrogen, this method was not successful. In 1922 Kamerlingh Onnes reached temperatures below $1K$ by reducing the vapor pressure above liquid helium to about $2*10^{-5}$ bar with a series of pumps [8]. The Joule–Thomson effect [42] is in this case the responsible for Onnes experiment to reach this low temperatures. The basic idea is that under suitable conditions a gas in expanding performs work against its internal forces. Basically

the gas is expanded through a small nozzle thermally isolated from its surroundings. The expansion under theses conditions takes place at constant enthalpy, since the expansion nozzle performs no work. following the next relation:

$$W = H_1 - H_2 = (U_1 + p_1V_1) - (U_2 + p_2V_2) \tag{1.1}$$

where H is the entalpy before and after, $U = \frac{3}{2}Nk_bT$ for ideal gases and $pV = Nk_bT$ [10]. Under Joule–Thomson effect conditions, $W = 0$ so $H_1 = H_2$, this expansion leads to a cooling or a warming and under certain conditions, becomes supersaturated. As a result, condensation takes place and a beam of clusters is formed.

Helium nanodroplets are typically produced by a continuous or pulsed adiabatic Expansion of pre−cooled helium through a small aperture from a reservoir into a vacuum [36]. In this process a droplet jet is formed, and its characteristics (blasting speeds and size distribution) can be changes due the manipulation of the set−up. For example, $\triangle$ pressure between the reservoir and the vacuum chamber (usually in the range of a few to $10MPa$) , the nozzle temperatures(from a few K to $T \leqslant 40K$) or the nozzle size (with pinholes of diameter rounding $5 - 20\mu m$).

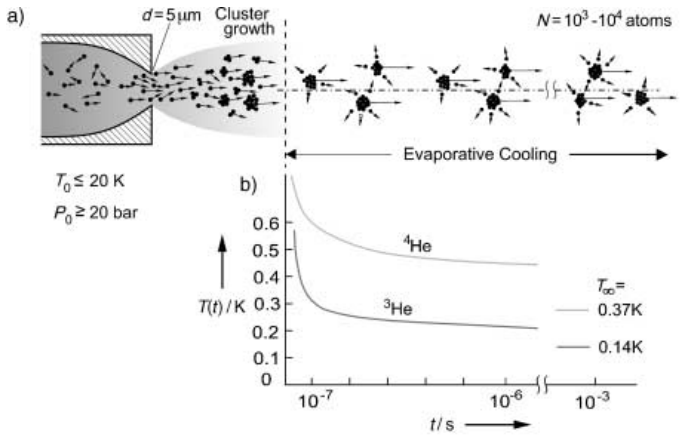

Figure 1.1: a) Schematic representation of the processes leading to the formation and subsequent cooling of helium droplets in a gas expansion. b) Calculated dependence of the droplet temperature on time for ^4He and ^3He droplets after they have left the cluster, taken from [41]

When the Helium expands from the nozzel, its thermal energy is transform in kinetic energy of a supersonic flow field. After the expantion into the vacuum, the gas becomes supersaturated and condensations starts to occurs, creating the beam clusters. This clusters are made of atoms or moleulces held togueter by Wannder wals fores, in this case He-He interaction, that share the same kinetic vector. This means that the two particules travel as close and parallel to each other that a

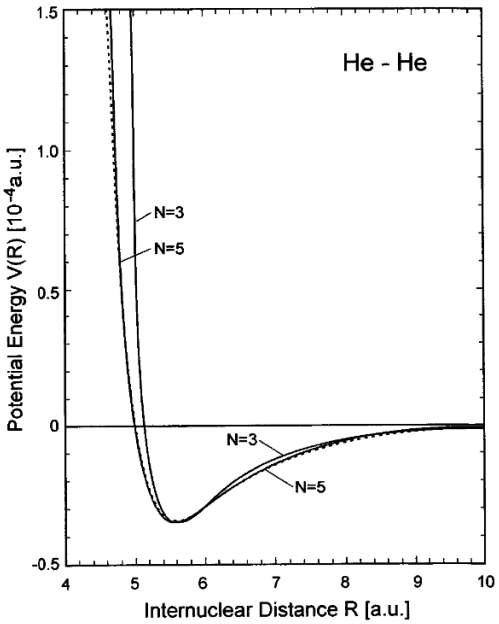

Figure 1.2: Waan der Wals potential for He-He interaction

bonding is possible, see fig 1.2. From the reference frame of the cluster, each of its molecules are close to cero movments, in He this enhace the conditions to be liquid and in consecience superfluidity is achive [16].

There is no mathematical approach of the physics behind this cooling expansion but usually, Raleigh scattering measurements in combination with an empirical scaling law [16] are used to estimate the mean cluster size giving a certain degree of control over the cluster size distribution by adjusting the nozzle width and the source pressure. The droplet size distribution during supersonic expansion in the follows a log-normal distribution of the form [18].

$$p(N) = \frac{1}{\sqrt{2\pi}N\sigma} \exp\left[-\frac{(ln(N/N_0)^2}{2\sigma^2}\right] \tag{1.2}$$

Where N is the number of atom in the cluster, σ is the distribution width and N_0 is the most likely numbers of atoms. Following it give a mean value.

$$\bar{N} = \exp\left(\mu + \frac{\sigma^2}{2}\right) \tag{1.3}$$

With a half width maxima of [18]

$$\sigma N_{\frac{1}{2}} = \exp\left(\mu - \sigma^2 + \sigma\sqrt{2ln(2)}\right) - \exp\left(\mu - \sigma^2 - \sigma\sqrt{2ln(2)}\right) \tag{1.4}$$

As show in Figure **??** The conditions in the He (pressure, temperature and nozzle

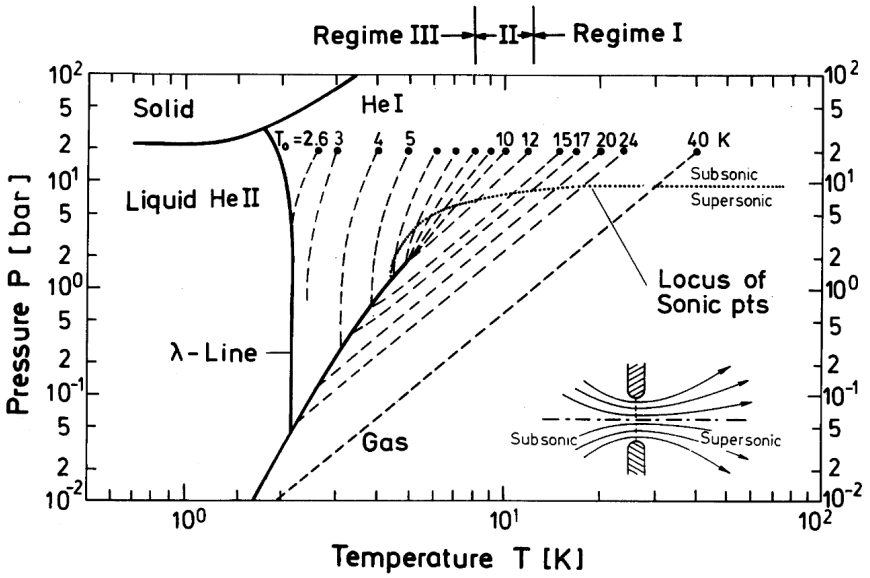

Figure 1.3: Expansion regimes. Pressure-Temperatur phase diagram for ^4He for Nozzle beam expansions starting from a stagnation of 20 bar and a temperatures. As dicusse, quialitatively different behaivors are shown for the regime I - II and II where starting in the gas phase, near the phase trnasition respectivelly. taken from [6].

size) in the free expansion will determine the characteristics of our final He beam. From Here three main regimes can be define.

Regime I or sub-critical expansion, begins in the gas phase and leads to droplet formation via condensation. this is the case of most expansions since the pressure are located below the critical pressure P_c. Regime II, also called as critical expansion, is basically and interminable regime that includes all trajectories which are near the critical point, leading to random expansion and difficult control of the beam due the large fluctuations in density. Regime III, the supercritical expansion, starts at low temperatures where the He stops behaving as an ideal gas, expecting flashing or cavitation breaking up the liquid drops jet. [6]

super-critical and sub-critical regimes have been studies in the last several years and are clearly identified in the resulting size distributions. Figure ?? shows that supercritical expansion forms large droplets (usually between $20-100nm$ diameter) while a sub-critical expansion is suited to generate small droplets (around $5-10nm$). A simple relation that can be done to calculate the size or number of atom in a Custer is using.

$$r = N_{1/3} * \rho A \tag{1.5}$$

Where r is the radius of the beam, ρ is the density, in thhis case of He $\rho =$

$0.0022A$ [37], but this approximation is not exact due the variation Of He density at this temperatures. As expected in both regimens for creating larger helium nano droplets, higher helium pressure and lower nozzle temperature are used. For our experiment a $5\mu m$ nozzle was used at temperature oscillating between $11 - 15K$, at pressure of $30to50$ bar.

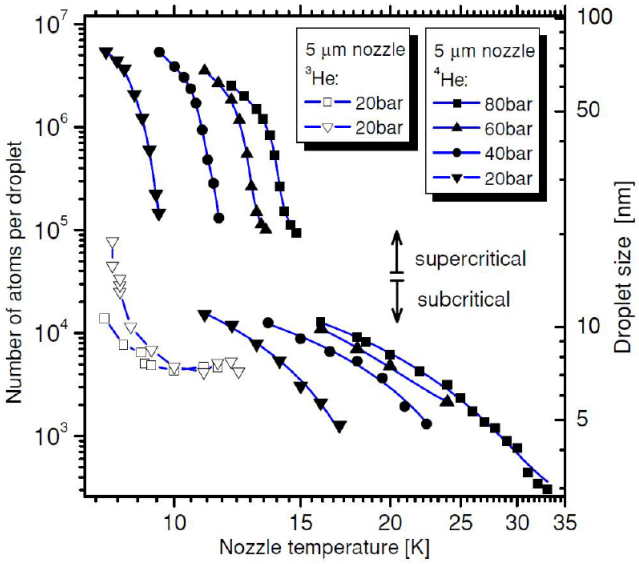

Figure 1.4: Sizes of the ^4He droplets as a function of nozzle temperature T and pressures, based on [40], using a $5\mu m$ nozzle. The su and super critical regimes are clearly diferenciated. Taken from [?]

1.1.1.2 Composite Clusters

We can define a composite cluster or doped cluster, as a atom bulk of one material that contains one or more different atomic elements. Usually in homogeneous clusters the main interest is their properties behaviour as a function of its size, but for doped clusters, the interaction between the elements creates new degrees of freedom that makes more complex its behaviour. For example, the new composite will have different structural properties due the spatial distribution of the species. Hence, composite clusters exhibit a more diverse behaviour and offer more opportunities to study different characteristics the material.

The first problem to overcome in composite cluster is how to create them. Two techniques can be used. The first one, is the co expansion of a previously mixed gas [39] or the He cluster is produced first and then crossed with an atomic beam of the doping species.

The first technique involves several technical problems, depends on possible interactions between the elements, the condensation ranges of the bulks and even in the affinity of the materials. One of the most used techniques, and the one used in this study is the one called pick-up technique [13]. The idea is simple, as well as a snowball on its way downhill collects or pick-up more snow. The He cluster, after being directional selected through a Skimmer, passes through a doping cell with a dopant gas at low densities ($102Pa$) [36]. As a result, the gas atoms that are along the droplet cross sections will be captured by the beam and travel with it. The probability for helium droplets to collect k atoms or molecules via inelastic collisions depends on the length of the oven cell l, the cross section of the droplets σ, and the particle density inside the cell n. As l and σ remains constant, varying the density in the doping cell can regulated the abundance of k, following the Poissonian statistics:

$$P_k(l, n, \sigma) = \frac{(ln\sigma)^k}{k!} e^{(-ln\sigma)} \tag{1.6}$$

Two important properties of these relation can be infer. First the maxima of different cluster sizes are equidistant, $n_{max} = \frac{k}{l\sigma}$ and second, the exponential function in equation becomes nearly one for small particle densities [5].

Every pick-up process leads to an energy transfer to the droplets. As the dopant rapidly cool down to their, it means a transfer of energy to the He causing an evaporaton of helium atoms to keep the temperature unchanged. This He evaporation or "shrinkage", leads to a decrease of the cross section of the droplet and the probability to collect a further particle is reduced. The involved energy is composed of the following contributions [5].

$$E = \langle E_{kin} \rangle + E_{in} + E_{binding} + E_{cluster} \tag{1.7}$$

where

$$\langle E_{kin} \rangle \approx \frac{3}{2} k_b T + \frac{1}{2} m v^2 \tag{1.8}$$

is the kinetic energy of the droplet depending on it mass and velocity and temperature in the gas cell.

At a certain energy entry, the complete droplet evaporates if to may dopping acces to it. With E_{kin} the average kinetic energy, E_{in} the internal. Several studies have studied the $E_{binding}$ with ^4He, given a broth number of materials to work with.. it also importat to take into acount that the binding energy include the cluste dopant binding as well as the dopant-dopant relation. [40]. Acommung energy bounding

for example $Xe - He$ is arround $26.9meV$ [25], or $He - H_2O$ is about $0.1eV$ [26], AA more detailed table of all the energy bounding energy used in this study can be found in the appendix.

1.2 Cluster-Intense Fields Interaction

To understanding of the interaction atoms-fields have been study broadly in physics since Einstein Photoionizasion Theory [9], that gives a base on all the quantum electrodynamics theory. The basics unders this theory is the behaivour of ligth as a electromagnetic field where the electron as a bounded charge in the atom can be afected. This quantum dynamic theory is well understood since 1957 for small atoms, with one, two or few electrons [2], but still big molecules and atoms have been challenging scientific for years. In this chapter we will give a brief introduction to the photoionization process, explaining at the same time multi-photoionization and tunnelling precesses, so we can finish with a more detailed presentation of Strong field interaction with clusters and the Keldish theory.

1.2.1 Photolonization for single atoms

The process of photoionization describes the leaving of an electron from its bound state into the continuum by interaction with electromagnetic field radiation [4]. The atomic bounded electrons while going through an electro magnetic field, in our case the laser beam, can absorb enough energy to get excited and fly away from the nucleus. A bound electron only can escape from an atom by absorbing photons its energy exceeds the binding energy of an electron [9]. When the photon energy of the laser is smaller than the ionization potential of the target, the electron can absorb two or more photos in the ionization process, this is called Multi photon ionization (MPI). Another possible process is called, tunnelling ionization, where due the quantum mechanic properties of the electrons under certain conditions absorb enough energy enough to be on an above threshold regime and due it quantum dynamic properties it can escape from it bounds via tunnelling.

There is a variety of theoretical approaches to describe interaction of laser fields with atoms. The Hamiltonian of the system of N particles (ions and electrons) with pair-wise Coulomb interactions under the action of an external time-dependent electric field has the form:

$$H = \sum_{1 \leqslant i \leqslant N} \frac{P_i}{2m_i} + \sum_{1 \leqslant i < j \leqslant N} \frac{q_i q_j}{\mid r_i - r_j \mid} + \sum_{1 \leqslant i \leqslant N}^{n} q_i r_i \varepsilon(t) \tag{1.9}$$

where r_{i,p_i} and q_i are the coordinates, momenta and charge of the particles including the interaction between the classical electric field and $\varepsilon(t)$ where [28]

$$\varepsilon(t) = \varepsilon_0 e_z cos(\omega t + \varphi) \tag{1.10}$$

The proces that drives ionization can be divide on two regimes, a quantum electrical regime and a clasical one. [21]. Equation 1.9, use the non-relativistic approximation and neglect contributions from magnetic fields. The classical description of the laser field is a good approximation for intense enough pulses, otherwise, quantum electrodynamics description is necessary.

An electron in the initial level with enery E_i can absorb an photon with energy $\hbar\omega$ leading to final transition where $E_f - E_i = \hbar\omega$, when the enrgy of the photon is larger than the bounding energy, or the Ionization barrier the elctron is free with a the remainin kinetic energy $E_{kin} = \hbar\omega - I_{pot}$ [1]. In classical mechanics the probability of the energy transition depends directly on the cross section (σ) of the electron in it was of the field However, in quantum mechanics, the photoionization cross section is related to the its transition probability between the initial and the final state given by Fermi's golden rule

$$W_{|i\rangle \to |f\rangle} = \frac{2\pi}{\hbar\hbar} |\langle f|H|i\rangle|^2 \delta(E_i - E_f - \hbar\omega) \tag{1.11}$$

$$\sigma(\hbar\omega) = \frac{2\pi}{3} \alpha a_{02} \hbar\omega |\langle f|r_n|i\rangle|^2 \tag{1.12}$$

When eq. 1.11 is thee transition probability of one lectron to jump from minitial state i to final state f, where H is the hamiltonian operator. Eq. 1.12 is the consequent cross sectiononsidering only the dipole part of the interaction Hamiltonian, where α is the fine structure coefficient, r_n is the position operador of the electron n [12].

Energy photon needed to ionize an atom is directly proportional to the the energetic distance between the electronic states and the ionization threshold. For states closer to the ionization potential a VUV photon can be enough to free a electron but for inner electrons higher photon energies are required, varying from several tens eV to the order of several tens of keV, needing radiation sources at shorter wavelengths such as XUV to X-rays. [1]

After photoionization is done, the electronic structure of the atom needs to rearrange via, due to the vacancy left by the ejected electron. Two relaxation processes can happens during this time. An electron from the outer shell will decay and replace the freed one, therefore the energy difference of the needs to be released in form of a

fluorescence photon or Auger electron. On one hand, in case of a fluorescence decay the ionic state of the target does not change, since no additional electron is release. on the other hand, the Auger decay is a non radiative relaxation process, where a second electron is released from the Coulomb potential of the ion.

In example. as shown in fig.... if an photon whit energy $\hbar\omega > E_{bin}$ ionized an electron, this will leave the atome lefting a gap. An electron in the higers level will replace the outer one, and lefting an ecxcess of energy. The outcome will be a fluerecence process with $E_{flu} = E_{in} - E_{out}$ or , the Auger $e-$, if $E_{in} - E_{out} > E_{bond}$ and this electron can also escape the atomic Coulomb potential [34].

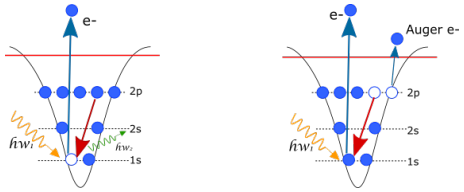

Figure 1.5: two example os the relaxation processes. On the left, A photon ionized an electron and the Electron Ein replaced, expelin a fluerecent photon in the process. on the rigth, the energie reliessed by the replacement electron is enougth to make another electron in the outer shell to also go to the continium, ASuger electron. taked form [32]

1.2.2 Multhiphoton and tunelling Ionization

Ionization is also possible even when one photon energy is lower than the binding potential. Laser fields with intensities below $I \leqslant 10^{14} W/cm^2$ are not strong enougth to change the binding potencial of an atom significantly [33] and is when mUltiphoton Ionization takes place (MPI). MPI is the simultaneous absorption of several photons to overcome the ionization barrier. The way MPI occurs depends on the laser frequency and intensity. When the intensity is much lower than the characteristic atomic resonance, MPI occurs via transitions through virtual states. Ionization by several photons at low laser intensities can be realized by the so-called resonance enhanced multiphoton ionization (REMPI) [27]. Ionization by a REMPI process takes place in two steps First, a resonant excitation by one or more photons takes place on an electron state of the atom. In the second step, this electron state is transformed into a virtual state, to an upper state until the electron is excited by spontaneous decay. So for example the total energy absorbed by an election until it gets ionizes is $n * \hbar\omega > I_{pot}$ where n is the number of photon absorbed until it actually have enough energy to overcome the potential I_{pot}

For Laser intensities $I > 10^{14} W/cm^2$, higher intensities and lower frequencies,

tunneling ionization (TI) is more likely to occur. In this case, the binding potential of the atom get is strongly afected by the electric fiels of the laser. Arround the peack of the electri field the potential gets narrower, and the electron in the outer states get closer to the bidding barrier, allowing the electron to tunneling througth the confining potential into de continium [15]. TI is inherently a quantum process. The bending of the Coulomb potential becomes by the superpossition of the coulomb potential and the laser field. Therefore TI must occure when the time of the ionization is shorter than a laser oscilation cycle [4]. Based in the same principle, when the Laser fiel becomes so strong to lower the binding potencial that separates the highest electron level, then the electrons in this state become free electrons. This process is called barrier suppression ionization or BSI [24].

In the fig **??**, we present a sketch of the 3 possible ionization processes explained above. On the left we present a simple ionization process where a photon with energy $E_{phot} = \hbar\omega$ is higher than the potential barrier. In the center a MPI process is shown, n photons exite the inner-shell electron, exiting it througth virtual level until it finally have enougth energy to be free to the continium. Finally on the left a TI happens. Here the coulomb potencia barrier is afectis by the laser files bending, the outter shell electron gets closets to it nuntil it tunnels [32].

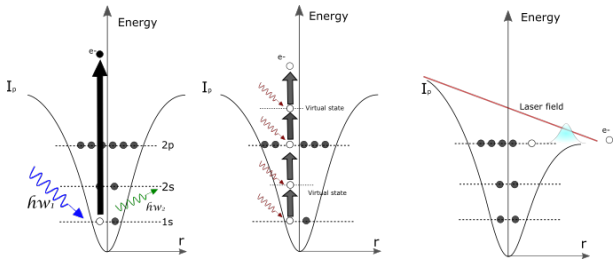

Figure 1.6: On the left is the scketch of a single photon ionization process, where a photon with energy $E_{phot} = \hbar\omega$ is higher than the potential barrier I_p. On the center the MPI process, inner-shell electron absorbs n photons, getting excited througth the electronic levels (reals or virtual) until it reach the continium. On the left the BSI Process, the coulomb potencial barrier bends by the laser fields, been lower than the outer shell electron state, the electrons can scape easilly. based on [32].

As explained the Intensity of the external fiel plays an important rol in the ionizaion process. A rather easy way to differenciate when each process needs to be taken into account is provides by the Keldysh parameter [22].

$$\gamma_k = \sqrt{\frac{I_p}{2U_p}} \tag{1.13}$$

Where γ_k is the Keldish parameter, I_p is the atoms ionization potential and U_p is

the ponderomotive potential defined as

$$U_p = \frac{e^2 E_0^2}{4 m_e \omega_0^2} \propto I\lambda^2 \tag{1.14}$$

where m_e is the mass of the electron, ω_0, λ, I and E_0 are the frequency, wavelength, intensity and the peak of the electric field of the laser pulse. On one hand, when the Keldish parameter is higher, $\gamma_k \gg 1$ MPI regime is consider. On the other hand, the $\gamma_k \ll 1$ describes the TI interaction.

1.2.3 kelysh Theory

in this section we will give abief introduction to keldysh theory andn the main repectutions for our work as the ionization rates. we where based this subchapter in the work of Keldy et all, [22], and the papers review of the theory by [30] and [21]. For a deeply explanation we recomend the reader to reference this works.

The keldysh Theory, also known as the Keldysh–Faisal–Reiss theroy (KFR), is well used for the description of quantum process induced by intense laser radiation. The applications and advantages of Keldysh formulation in many-body theory among can over come from, treatment of systems away from thermal equilibrium (with or wothpout presence of external fields), solutions in supersymmetry methods of systems with quenched disorder to the calculation of the full counting statistics of a quantum observable [19].

According to the Keldysh ansatz, the transition probability amplitude between an atomic bound state and the continuum by the value of the photoelectron momentum p measured at the detector is given by: [30].

$$M_k(p) = -\frac{i}{\hbar} \int_{\inf}^{+\inf} \langle \Phi_p \mid V_{int}(t) \mid \Phi_0 \rangle dt \tag{1.15}$$

Where M_k denotes the Keldys transition probability, Φ_0 is the bond state wave funtion unperturbed and Φ_p is the caonical momentum equal to p, also known as the Volkov Funtion, and V_{int} is the electron field interaction operator. If the amplitude of ionization $M_k(p)$ is known the differential probability to find the photoelectron in the elementary volume near the momentum p is givwen by the momentum distribution of the photoelectrons

$$dW(p) = \mid M(p) \mid^2 d^3p \tag{1.16}$$

givin a total probability of

$$W = \int \mid M(p) \mid^2 d^e p \tag{1.17}$$

meaning thet for enougth long pulses containing a large number of optical periods so that its electromagnetic field is close to a periodical function of time close to the initial, it is physically more appropriate to use probabilities per time unit (rates) instead of time-integrated values. .

.

.

.

.

.

.

1.2.4 Ponderomative enery

As soon as an electron is release into the continuum, it is under the influence of the external laser field. A description of the energy that it acquires during this interaction is given by the ponderomotive energy (PE).

$$U_p = \frac{e_2 E_a^2}{4m\omega^2} \tag{1.18}$$

Where m and e is the electron mass and charge, E_a and ω_0 amplitude and frequency of the electric field respectively. The formula of the ponderomotive force can be easyly derived as shown in [31] [7]. Lets consider a polarized electric field (in a.u).

$$E = \widehat{z} E_a sin(\omega_0 t) \tag{1.19}$$

considering only the $\widehat{z}$-components so we can avoid the vector sign. by classical mechanics we have.

$$p(t) = -\int_{t_0}^{t} E(t)dt = \frac{E_0}{\omega}(cos(\omega_0 t) - cos(\omega_0 t_0)) \tag{1.20}$$

The term at the left of the parenthesis is knows as the time varying Quiver terms, and on the one on the right, reefers to the drift motion. turning our fields in terms of vector potential we will have

$$E(t) = \frac{\delta A(t)}{\delta t} \tag{1.21}$$

$$p(\infty) = A(t_0) = -\int_{-\infty}^{t} E(t)dt = \frac{E_0}{w}cos(w_0 t_0)$$

(1.22)

so in the case where the pulse duration is big $t \longrightarrow \infty$ the $p + A(t) = 0$. This means that the momentum acquired by the electron will depends on the phase it is realized wt. Since the electron can be unbound in any phase of the laser pulse, will have an average kinetic energy described by

$$U_p = \frac{1}{2\pi}\int(-\frac{E}{w}cos(wt))^2 d(wt) = \frac{E_0^2}{4w_0^2} = \frac{{p_{max}}^2}{2}$$

(1.23)

The pondemorotive energy also gives the maximum momentum that an electron can acquire (eq. 1.2.4), given at the maxima . The ωt phase relation, defines what its called*the three step model* showed in figure . The first step correspond to $\omega t < \pi/2$ where the laser field is suppress, and as explained above, TI or BSI can take place. The second step, is where $\omega t > 3\pi/2$, on contrary step 1 the potential barrier is enhance, electron in the continuum that was winning kinetic energy is catched by the potential again, driven back to the atom. Finally the step 3 at phase $\omega t = n * \pi$, for $n01, 2, 3....$ At $n = 2$ it is called "recollision process" of the electron. Where the electron can be catch by the potential again, and the excess of energy cause realising another bound electrons depending on the kinetic energy necessary [23]

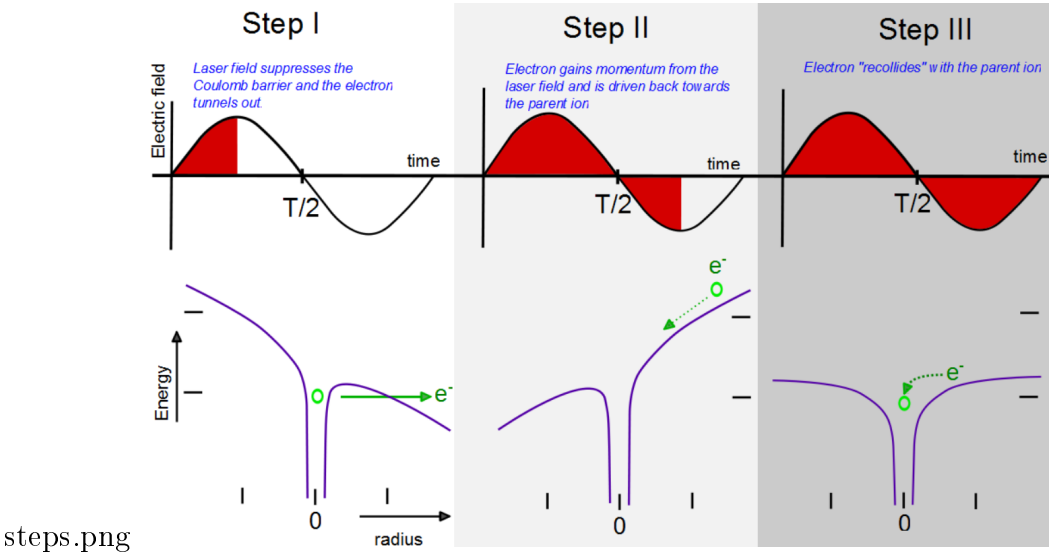

steps.png

Figure 1.7: Recollision process at the three step model. Taken from [24]

If we transform the eq. 1.2.4 to laser intensities we will have $U_p = 9,33 * 10^{-14} I[W * cm^{-2}] * \lambda^2[]$. For a MIR-pulse with intensities $\sim 10^{14}[W/cm^2]$ and $\lambda \sim 3200[nm]$ we

have electron energies between one and hundred of eV.

It is helpful to divide the process of intense laser-cluster interaction into three stages (Saalmann et al., 2006). At the first stage, called "atomic ionization", pulse atoms are ionized independently of each other by the electric field at leading edge of the laser pulse. Ionization at this stage is called inner ionization and occurs mainly through tunnelling or barrier suppression. Some of the ionized electrons acquire positive total energy and leave the cluster, i. e. they undergo outer ionization. Other ionized electrons stay inside the cluster attracted to its positive ion background. Since they are free to travel inside the cluster volume, they are called quasi-free (Last and Jortner, 1999). Thus, after the first stage and the cluster nanoplasma is formed that consists of ions and quasi-free electrons. At the second stage the nanoplasma expands while still interacting with the laser field. A number of processes responsible for energy absorption take place at this stage. Ions are further ionized by a combined force of the laser and other ions [ionization ignition (Rose-Petruck et al., 1997)]. Quasi-free electrons oscillate driven by the laser pulse and are heated to high temperatures. The heating becomes extremely efficient and leads to significant outer ionization when the collective oscillations of quasi-free electrons become resonant with the laser pulse (plasma resonance, see Sec. 2.3.2 below). At the third stage, when the laser pulse has ceased, the ions continue to expand. Then, the cluster potential becomes shallower, resulting in the rise of potential barriers between the ions and thus hindering inner ionization. However, this makes it easier for the hot quasi-free electrons to leave the cluster. Quasi-free electrons that reside inside the cluster recombine with the ions producing x rays. At this stage experimentally observable distributions of particles are formed. Now we discuss in more details how the energy absorption takes place.

List of Figures

1.1 Scheme for a nozzle expansion 9
1.2 Waan der Wall He-He potential 10
1.3 Phase diagram for Expantion regimens 11
1.4 Expantion droplets Regimens 12
1.5 Relaxation processes for photoionization 16
1.6 Ionization regimes 17
1.7 Ponderomotive 3 steps 20

List of Tables

2 Bibliography

[1] Becker, U. (Hrsg.) ; Shirley, D. A. (Hrsg.): *VUV and Soft X-Ray Photoionization*. http://dx.doi.org/10.1007/978-1-4613-0315-2

[2] A. Bethe, H. ; E. Salpeter, E. : *The Quantum Mechanics of One- and Two-Electron Atoms*. Bd. 35. http://dx.doi.org/10.1007/978-3-662-12869-5. http://dx.doi.org/10.1007/978-3-662-12869-5

[3] Atkins, K. R.: *Liquid Helium*. Cambridge University Press. – ISBN 978–1–107–63890–7. – Google-Books-ID: gzmNAwAAQBAJ

[4] Berkowitz, J. : *Photoabsorption, photoionization, and photoelectron spectroscopy*. Academic Press. – ISBN 978–0–12–091650–4. – Google-Books-ID: POeHAAAAIAAJ

[5] Bünermann, O. ; Stienkemeier, F. : Modeling the formation of alkali clusters attached to helium nanodroplets and the abundance of high-spin states. 61, Nr. 3, 645–655. http://dx.doi.org/10.1140/epjd/e2011-10466-0. – DOI 10.1140/epjd/e2011–10466–0. – ISSN 1434–6079

[6] Buchenau, H. ; Knuth, E. L. ; Northby, J. ; Toennies, J. P. ; Winkler, C. : Mass spectra and time-of-flight distributions of helium cluster beams. 92, Nr. 11, 6875–6889. http://dx.doi.org/10.1063/1.458275. – DOI 10.1063/1.458275. – ISSN 0021–9606, 1089–7690

[7] Connerade, J. P.: *Highly Excited Atoms*. Cambridge University Press. – ISBN 978–0–521–43232–0. – Google-Books-ID: VgpkXDfkqYEC

[8] Delft, D. van ; Kes, P. : The discovery of superconductivity. 63, Nr. 9, 38–43. http://dx.doi.org/10.1063/1.3490499. – DOI 10.1063/1.3490499. – ISSN 0031–9228

[9] Einstein, A. : Über einen die Erzeugung und Verwandlung des Lichtes betreffenden heuristischen Gesichtspunkt. 322, Nr. 6, 132–148. http://dx.doi.org/10.1002/andp.19053220607. – DOI 10.1002/andp.19053220607. – ISSN 1521–3889

[10] Enss, C. ; Hunklinger, S. : *Low-Temperature Physics*. Springer-Verlag //www.springer.com/de/book/9783540231646. – ISBN 978–3–540–23164–6

[11] Fennel, T. ; Meiwes-Broer, K.-H. ; Tiggesbäumker, J. ; Reinhard, P.-G. ; Dinh, P. M. ; Suraud, E. : Laser-driven nonlinear cluster dynamics. 82, Nr. 2, 1793–1842. http://dx.doi.org/10.1103/RevModPhys.82.1793. – DOI 10.1103/RevModPhys.82.1793

[12] Fermi, E. : Quantum Theory of Radiation. 4, Nr. 1, 87–132. http://dx.doi.org/10.1103/RevModPhys.4.87. – DOI 10.1103/RevModPhys.4.87

[13] Gough, T. E. ; Mengel, M. ; Rowntree, P. A. ; Scoles, G. : Infrared spectroscopy at the surface of clusters: SF6 on Ar. 83, Nr. 10, 4958–4961. http://dx.doi.org/10.1063/1.449757. – DOI 10.1063/1.449757. – ISSN 0021–9606

[14] Grebenev, S. ; Toennies, J. P. ; Vilesov, A. F.: Superfluidity Within a Small Helium-4 Cluster: The Microscopic Andronikashvili Experiment. 279, Nr. 5359, 2083–2086. http://dx.doi.org/10.1126/science.279.5359.2083. – DOI 10.1126/science.279.5359.2083. – ISSN 0036–8075, 1095–9203

[15] Griffiths, D. J.: *Introduction to electrodynamics*. Fourth edition. Pearson. – ISBN 978–0–321–85656–2

[16] Hagena, O. F. ; Obert, W. : Cluster Formation in Expanding Supersonic Jets: Effect of Pressure, Temperature, Nozzle Size, and Test Gas. 56, Nr. 5, 1793–1802. http://dx.doi.org/10.1063/1.1677455. – DOI 10.1063/1.1677455. – ISSN 0021–9606

[17] Halperin, W. P. ; Rasmussen, F. B. ; Archie, C. N. ; Richardson, R. C.: Properties of melting 3He: Specific heat, entropy, latent heat, and temperature. 31, Nr. 5, 617–698. http://dx.doi.org/10.1007/BF00116046. – DOI 10.1007/BF00116046. – ISSN 1573–7357

[18] Harms, J. ; Toennies, J. P. ; Dalfovo, F. : Density of superfluid helium droplets. 58, Nr. 6, 3341–3350. http://dx.doi.org/10.1103/PhysRevB.58.3341. – DOI 10.1103/PhysRevB.58.3341

[19] Kamenev, A. : Introduction to the Keldysh Formalism.

[20] Kapitza, P. : Viscosity of Liquid Helium below the -Point. 141, Nr. 3558, 74. http://dx.doi.org/10.1038/141074a0. – DOI 10.1038/141074a0. – ISSN 1476–4687

[21] Karnakov, B. M. ; Mur, V. D. ; Popruzhenko, S. V. ; Popov, V. S.: Strong field ionization by ultrashort laser pulses: Application of the Keldysh theory. 374, Nr. 2, 386–390. http://dx.doi.org/10.1016/j.physleta.2009.10.058. – DOI 10.1016/j.physleta.2009.10.058. – ISSN 0375–9601

[22] KELDYSH, L. V.: Ionization in the field of a strong electromagnetic wave. 20, 1307. https://ci.nii.ac.jp/naid/10006486551/

[23] Krishnan, S. R. ; Fechner, L. ; Kremer, M. ; Sharma, V. ; Fischer, B. ; Camus, N. ; Jha, J. ; Krishnamurthy, M. ; Pfeifer, T. ; Moshammer, R. ; Ullrich, J. ; Stienkemeier, F. ; Mudrich, M. : Ignition of Doped Helium Nanodroplets in Intense Few-Cycle Laser Pulses. In: Yamanouchi, K. (Hrsg.) ; Katsumi, M. (Hrsg.): *Multiphoton Processes and Attosecond Physics*, Springer Berlin Heidelberg (Springer Proceedings in Physics). – ISBN 978–3–642–28948–4, S. 385–390

[24] Krishnan, S. R.: Doped helium nanodroplets in intense few-cycle infrared pulses. http://inis.iaea.org/Search/search.aspx?orig_q=RN:43095633

[25] Lewerenz, M. ; Schilling, B. ; Toennies, J. P.: Successive capture and coagulation of atoms and molecules to small clusters in large liquid helium clusters. 102, Nr. 20, 8191–8207. http://dx.doi.org/10.1063/1.469231. – DOI 10.1063/1.469231. – ISSN 0021–9606

[26] Lewis, W. K. ; Harruff-Miller, B. A. ; Leatherman, P. ; Gord, M. A. ; Bunker, C. E.: Helium droplet calorimetry of strongly bound species: Carbon clusters from C_2 to C_{12}. 85, Nr. 9, 094102. http://dx.doi.org/10.1063/1.4895670. – DOI 10.1063/1.4895670. – ISSN 0034–6748, 1089–7623

[27] Mainfray, G. : MULTIPHOTON IONIZATION OF ATOMS.

[28] Mikaberidze, A. : *Atomic and molecular clusters in intense laser pulses.* https://www.pks.mpg.de/mpi-doc/rostgruppe/dissertation/mikaberidze_dissertation.pdf

[29] Nauta, K. ; Miller, R. E.: Nonequilibrium Self-Assembly of Long Chains of Polar Molecules in Superfluid Helium. 283, Nr. 5409, 1895–1897. http://dx.doi.org/10.1126/science.283.5409.1895. – DOI 10.1126/science.283.5409.1895. – ISSN 0036–8075, 1095–9203

[30] Popruzhenko, S. V.: Keldysh theory of strong field ionization: history, applications, difficulties and perspectives. 47, Nr. 20, 204001. http://dx.doi.org/

10.1088/0953-4075/47/20/204001. – DOI 10.1088/0953–4075/47/20/204001. – ISSN 0953–4075

[31] Protopapas, M. ; Keitel, C. H. ; Knight, P. L.: Atomic physics with super-high intensity lasers. 60, Nr. 4, 389–486. http://dx.doi.org/10.1088/0034-4885/60/4/001. – DOI 10.1088/0034–4885/60/4/001. – ISSN 0034–4885, 1361–6633

[32] Rafipoor, A. J. M.: *Two-Color Photoionization Experiments with Ultrashort Light Pulses on Small Atomic Systems*

[33] Rhodes, C. K.: Multiphoton Ionization of Atoms. 229, Nr. 4720, 1345–1351. http://dx.doi.org/10.1126/science.229.4720.1345. – DOI 10.1126/science.229.4720.1345. – ISSN 0036–8075, 1095–9203

[34] Schmidt, V. : *Electron Spectrometry of Atoms using Synchrotron Radiation*. Cambridge University Press. – ISBN 978–0–521–55053–6

[35] Stebbings, S. L. ; Süssmann, F. ; Yang, Y.-Y. ; Scrinzi, A. ; Durach, M. ; Rusina, A. ; Stockman, M. I. ; Kling, M. F.: Generation of isolated attosecond extreme ultraviolet pulses employing nanoplasmonic field enhancement: optimization of coupled ellipsoids. 13, Nr. 7, 073010. http://dx.doi.org/10.1088/1367-2630/13/7/073010. – DOI 10.1088/1367–2630/13/7/073010. – ISSN 1367–2630

[36] Stienkemeier, F. ; Lehmann, K. K.: Spectroscopy and dynamics in helium nanodroplets. 39, Nr. 8, R127–R166. http://dx.doi.org/10.1088/0953-4075/39/8/R01. – DOI 10.1088/0953–4075/39/8/R01. – ISSN 0953–4075, 1361–6455

[37] Stringari, S. ; Treiner, J. : Systematics of liquid helium clusters. 87, Nr. 8, 5021–5027. http://dx.doi.org/10.1063/1.452818. – DOI 10.1063/1.452818. – ISSN 0021–9606

[38] Swenson, C. A.: The Liquid-Solid Transformation in Helium near Absolute Zero. 79, Nr. 4, 626–631. http://dx.doi.org/10.1103/PhysRev.79.626. – DOI 10.1103/PhysRev.79.626

[39] Tchaplyguine, M. ; Lundwall, M. ; Gisselbrecht, M. ; Öhrwall, G. ; Feifel, R. ; Sorensen, S. ; Svensson, S. ; Mårtensson, N. ; Björneholm, O. : Variable surface composition and radial interface formation in

self-assembled free, mixed ArXe clusters. 69, Nr. 3, 031201. http://dx.doi.org/10.1103/PhysRevA.69.031201. – DOI 10.1103/PhysRevA.69.031201

[40] Toennies, J. P. ; Vilesov, A. F.: Spectroscopy of Atoms and Molecules in Liquid Helium. 49, Nr. 1, 1–41. http://dx.doi.org/10.1146/annurev.physchem.49.1.1. – DOI 10.1146/annurev.physchem.49.1.1

[41] Toennies, J. P. ; Vilesov, A. F.: Superfluid Helium Droplets: A Uniquely Cold Nanomatrix for Molecules and Molecular Complexes. 43, Nr. 20, 2622–2648. http://dx.doi.org/10.1002/anie.200300611. – DOI 10.1002/anie.200300611. – ISSN 1521–3773

[42] Weinberger, P. : The discovery of thermodynamics. 93, Nr. 20, 2576–2612. http://dx.doi.org/10.1080/14786435.2013.784402. – DOI 10.1080/14786435.2013.784402. – ISSN 1478–6435

[43] Whittle, E. ; Dows, D. A. ; Pimentel, G. C.: Matrix Isolation Method for the Experimental Study of Unstable Species. 22, Nr. 11, 1943–1943. http://dx.doi.org/10.1063/1.1739957. – DOI 10.1063/1.1739957. – ISSN 0021–9606, 1089–7690

[44] Zhao, K. ; Zhang, Q. ; Chini, M. ; Wu, Y. ; Wang, X. ; Chang, Z. : Tailoring a 67 attosecond pulse through advantageous phase-mismatch. 37, Nr. 18, 3891–3893. http://dx.doi.org/10.1364/OL.37.003891. – DOI 10.1364/OL.37.003891. – ISSN 1539–4794

Danksagung

An dieser Stelle Danke

Erklärung

Hiermit versichere ich, die e ingereichte Arbeit selbständig verfasst und keine anderen als die von mir angegebenen Quellen und Hilfsmittel benutzt zu haben. Wörtlich oder inhaltlich verwendete Quellen wurden entsprechend den anerkannten Regeln wissenschaftlichen Arbeitens (lege artis) zitiert. Ich erkläre weiterhin, dass die vorliegende Arbeit noch nicht anderweitig eingereicht wurde.

Ort, Datum ..... Unterschrift .....